van der Waals coefficients for alkali-metal atoms in material media

Bindiya Arora[1,*] and B. K. Sahoo[2,†]

[1]*Department of Physics, Guru Nanak Dev University, Amritsar, Punjab 143005, India*

[2]*Theoretical Physics Division, Physical Research Laboratory, Navrangpura, Ahmedabad 380009, India*

(Received 10 July 2013; revised manuscript received 2 January 2014; published 18 February 2014)

The C_3 coefficients and their ratios for the alkali-metal atoms are determined very accurately by taking into account the optical properties of the atoms and four distinct types of trapping materials such as Au (metal), Si (semiconductor), vitreous SiO_2 (dielectric), and SiN_x (dielectric). Dynamic dipole polarizabilities are calculated precisely for the alkali-metal atoms that produce C_3 coefficients in a perfectly conducting medium within 0.2% accuracy. Thus, uncertainties from the atomic polarizabilities in the evaluation of the material-dependent C_3 coefficients are small and accuracies of these C_3 values mainly rely on the used optical data which are not taken into account in the present work. Our findings are in very good agreement with the available measurements, but they differ by around 10% from the previously reported high-precision calculations in heavy atoms for the perfect conductors. We also revisit the dispersion coefficients for the alkali-metal dimers and evaluate them using the above dynamic dipole polarizabilities which provide slightly different error bars than the other reported precise results. These coefficients are fitted into a ready-to-use functional form to aid the experimentalists in finding out the interaction potential only with the knowledge of atom-wall distance.

DOI: 10.1103/PhysRevA.89.022511 PACS number(s): 31.30.jh, 34.35.+a, 31.15.ap, 31.50.Bc

I. INTRODUCTION

Accurate information on the long-range interactions such as dispersion (van der Waals) and retarded (Casimir-Polder) potentials between two atoms and between an atom and surface of the trapping material are necessary for the investigation of the underlying physics of atomic collisions especially in the ultracold atomic experiments [1–4]. Atom-surface interactions may lead to a shift in the oscillation frequency of the trap which alters the trapping frequency as well as magic wavelengths for state-insensitive trapping of the trapped condensate [5]. Moreover, this effect has also gained interest in generating novel atom optical devices known as the "atom chips" [6]. In addition, the knowledge of dispersion coefficients is required in experiments of photoassociation, fluorescence spectroscopy, determination of scattering lengths, analysis of Feshbach resonances, determination of stability of Bose-Einstein condensates (BECs), probing extra dimensions to accommodate Newtonian gravity in quantum mechanics, etc. [7–13].

There has been much experimental evidence of an attractive force between neutral atoms and between neutral atoms with trapping surfaces but their precise determinations are very difficult [14–16]. Instead, precise measurements of their ratios have been reported recently [17,18]. In the past two decades, several groups have calculated the dispersion coefficients defining interaction between an atom and a wall using various many-body approaches [19–26] without giving their probable uncertainties. More importantly the high-precision results are provided for a perfect conducting wall by evaluating the principal electric dipole ($E1$) matrix elements using a relativistic coupled-cluster (RCC) method at the linear approximation (SD method) and calculating the core and core-valence correlation contributions to the dipole polarizabilities using a relativistic random phase approximation (RRPA method) and Dirac-Fock (DF) method, respectively [19,20]; however the atom-wall interaction potentials are known to be highly dependent on the dielectric properties of the materials [23–25] and evaluation of these dispersion coefficients is very complex [5,26–29]. Using the Lifshitz theory [1,30], the dispersion coefficients are expressed in terms of the conducting properties of the medium and the dynamic polarizabilities of the atoms [23,28,29,31]. In some of the earlier studies, the material dependent dispersion coefficients have been evaluated using either less accurate dipole polarizabilities or considering them from elsewhere [16,23,24].

In the present work, we determine the dispersion coefficients for the alkali-metal atoms considering the trapping material as a good conductor like Au, a semi-conductor like Si and dielectric objects like SiO_2 and SiN_x. The quality of the results have been improved by employing more accurate values of the dynamic polarizabilities which are evaluated using a number of $E1$ matrix elements extracted from the precise measurements of the lifetimes and static dipole polarizabilities of few low-lying states of the considered atoms and determining other important $E1$ matrix elements considering nonlinear terms in the RCC theory. Unless stated otherwise, we give all the physical quantities in atomic units (a.u.) throughout the paper.

II. THEORY

Casimir and Polder had estimated that at intermediately large separations, the retardation effects of the virtual photons passing between an atom and its image weakens the attractive atom-wall force and the force scales with a different power law [2]. In this scenario, the atom-surface interaction potential resulting from the fluctuating dipole moment of an atom interacting with its image in the surface is given by [1,23,30]

$$U^a(R) = -\frac{\alpha_{fs}^3}{2\pi}\int_0^\infty d\omega\omega^3\alpha(\iota\omega)\int_1^\infty d\xi e^{-2\alpha_{fs}\xi\omega R}H(\xi,\epsilon(\iota\omega)), \quad (1)$$

*arorabindiya@gmail.com

†bijaya@prl.res.in

where α_{fs} is the fine-structure constant, $\epsilon(\omega)$ is the frequency-dependent dielectric constant of the wall, R is the distance between the atom and the surface, and $\alpha(\iota\omega)$ is the ground-state dynamic polarizability with imaginary argument. The function $H(\xi,\epsilon(\iota\omega))$ is given by

$$H(\xi,\epsilon) = (1-2\xi^2)\frac{\xi'-\epsilon\xi}{\xi'+\epsilon\xi} + \frac{\xi'-\xi}{\xi'+\xi}, \tag{2}$$

with $\xi' = \sqrt{\xi^2+\epsilon-1}$.

The complexity in the determination of Eq. (1) lies in the evaluation of $H(\xi,\epsilon)$ which is a function of the dielectric permittivity of the material wall. In a simple approximation of the medium being a perfect conductor for which $\epsilon(\omega)\to\infty$, it yields [22]

$$U^a(R) = -\frac{C_3}{R^3} f_3(R), \tag{3}$$

where

$$f_3(R) = \frac{1}{4\pi C_3}\int_0^\infty d\omega\alpha(\iota\omega)e^{-2\alpha_{fs}\omega R}P(\alpha_{fs}\omega R) \tag{4}$$

for $P(x) = 2x^2+2x+1$.

In fact, Eq. (3) at the short distances becomes [2]

$$U^a(R) = -\frac{1}{4\pi R^3}\int_0^\infty d\omega\alpha(i\omega)\frac{\epsilon(i\omega)-1}{\epsilon(i\omega)+1}, \tag{5}$$

which for a perfect conducting medium ($\frac{\epsilon(\iota\omega)-1}{\epsilon(\iota\omega)+1}\to 1$) further simplifies to

$$U^a(R) = -\frac{C_3}{R^3} \tag{6}$$

with the short-distance dispersion coefficient C_3. In other realistic materials with their refractive indices $n=\sqrt{\epsilon}$ varying between 1 and 2, $\frac{\epsilon(\iota\omega)-1}{\epsilon(\iota\omega)+1}\approx\frac{\epsilon(0)-1}{\epsilon(0)+1}$ is nearly a constant and can be approximated to 0.77 [14]. For more preciseness, it is necessary to consider the actual frequency dependencies of ϵs in the materials to determine the C_3 values.

At the asymptotic region, where the approximations $\alpha(\iota\omega)\approx\alpha(0)$, $\epsilon(\iota\omega)\approx\epsilon(0)$ and for the frequency dependent magnetic permeability $\mu(\iota\omega)\approx\mu(0)$ are valid, we get [31]

$$U^a(R) = -\frac{C_4}{R^4} \tag{7}$$

with the long-distance dispersion coefficient C_4, which for the magnetic materials is given by

$$C_4 = \frac{3\alpha(0)}{16\pi\alpha_{fs}}\int_1^\infty dv\left[\left(\frac{2}{v^2}-\frac{1}{v^4}\right)\times\frac{\epsilon(0)v-\sqrt{\epsilon(0)\mu(0)-1+v^2}}{\epsilon(0)v+\sqrt{\epsilon(0)\mu(0)-1+v^2}}\times\frac{1}{v^2}\frac{\mu(0)v-\sqrt{\epsilon(0)\mu(0)-1+v^2}}{\mu(0)v+\sqrt{\epsilon(0)\mu(0)-1+v^2}}\right], \tag{8}$$

and in the nonmagnetic materials, this is simplified to

$$C_4 = \frac{3\alpha(0)}{16\pi\alpha_{fs}}\int_1^\infty dv\left[\left(\frac{2}{v^2}-\frac{1}{v^4}\right)\times\frac{\epsilon(0)v-\sqrt{\epsilon(0)-1+v^2}}{\epsilon(0)v+\sqrt{\epsilon(0)-1+v^2}}\times\frac{1}{v^2}\frac{v-\sqrt{\epsilon(0)-1+v^2}}{v+\sqrt{\epsilon(0)-1+v^2}}\right] \tag{9}$$

for the integration variable v as a function of velocity of light. In a perfectly conducting medium, this turns out to be

$$C_4 = \frac{3\alpha(0)}{8\pi\alpha_{fs}}\frac{\epsilon(0)-1}{\epsilon(0)+1}. \tag{10}$$

This is given in a more general form as

$$U^a(R) = -\frac{C_4}{R^3(R+\lambda\!\!\!^{-})}f_4(R) \tag{11}$$

to account the retardation effects in the evaluation of the interaction potential of a material medium with the reduced wavelength $\lambda\!\!\!^{-}$.

It would be interesting to test the validity of both the approximations given by Eqs. (3) and (11) by evaluating the C_3, C_4, $f_3(R)$, and $f_4(R)$ quantities together for different atoms in the real conducting (metal), semiconducting, and dielectric materials. Since evaluation of the C_3 coefficients requires only the knowledge of the Planck's constant whereas evaluation of the C_4 coefficients requires velocity of light [31], we choose to determine only the C_3 coefficients and $f_3(R)$ here. By converting the results for the above complex quantities to a known functional form, it would be useful for reproducing the interaction potentials easily at any given distances for practical use.

In the present work, four distinct materials such as Au, Si and SiO_2, and SiN_x belonging to conducting, semiconducting, and dielectric objects are considered to find out $f_3(R)$ functions explicitly combining expressions given by Eqs. (1), (3), and (5). Finally, these results are compared against the results obtained for the perfect conductor to demonstrate their differences.

Similarly, the leading term in the long-range interaction between two atoms denoted by a and b is approximated by $U^{ab}(R) = -\frac{C_6^{ab}}{R^6}$, where the C_6^{ab} is known as the van der Waals coefficient and R is the distance between two atoms. If retardation effects are included then it is modified to $U^{ab}(R) = -\frac{C_6^{ab}}{R^6}f_6^{ab}(R)$. The dispersion coefficient C_6^{ab} and the damping coefficient $f_6^{ab}(R)$ between the atoms can be estimated using the expressions [22]

$$C_6^{ab} = \frac{3}{\pi}\int_0^\infty d\omega\alpha^a(\iota\omega)\alpha^b(\iota\omega)$$

and

$$f_6^{ab} = \frac{1}{\pi C_6^{ab}}\int_0^\infty d\omega\alpha^a(\iota\omega)\alpha^b(\iota\omega)e^{-2\alpha_{fs}\omega R}Q(\alpha_{fs}\omega R),$$

where $Q(x) = x^4+2x^3+5x^2+6x+3$.

III. METHOD OF CALCULATIONS

The real values of the dielectric constants at the imaginary frequencies are obtained by using the Kramers-Kronig formula [32]

$$\epsilon(\iota\omega) = 1 + \frac{2}{\pi}\int_0^\infty d\omega' \frac{\omega' \mathrm{Im}[\epsilon(\omega')]}{\omega^2 + \omega'^2}. \tag{12}$$

The dielectric functions of the materials can be conveniently approximated to [26]

$$\epsilon(\iota\omega) = 1 - \left(\frac{\omega_p}{\omega}\right)^2 \tag{13}$$

in the plasma model or in more accurate form as

$$\epsilon(\iota\omega) = 1 - \frac{\omega_p^2}{\omega(\omega + \iota\gamma)} \tag{14}$$

in the Drude model, where ω_p and γ are known as the plasma frequency and Drude relaxation rate, respectively. For Au, the typical values used in the above expressions are around $\omega_p = 9.02$ eV and $\gamma = 0.035$ eV [23,26]. These quantities can be evaluated within a reasonable accuracy using the Drude-Lorentz function

$$\epsilon(\iota\omega) = \epsilon(\iota\infty) + \frac{[\epsilon(\iota 0) - \epsilon(\iota\infty)]\omega_0^2}{\omega^2 + \omega_0^2}, \tag{15}$$

with a cutoff frequency ω_0 from where onwards $\epsilon(\iota\omega)$ values remain almost constant.

To obtain more physical results, we evaluate the imaginary parts of the dielectric constants using the relation

$$\mathrm{Im}\,[\epsilon(\omega)] = 2\mathrm{n}(\omega)\kappa(\omega), \tag{16}$$

where $n(\omega)$ and $\kappa(\omega)$ are the real and imaginary parts of the refractive index of a material at frequency ω. Experimental data for $n(\omega)$ and $\kappa(\omega)$ of the considered materials are listed in [33] against a finite set of ω's except for SiN_x. We use the Tauc-Lorentz model [16,32] for estimating the dielectric constants of SiN_x. Substituting the $\mathrm{Im}\,[\epsilon(\omega)]$ values in the Kramers-Kronig formula [Eq. (12)], we evaluate $\epsilon(\iota\omega)$ values to use them in the determination of the C_3 coefficients.

For the numerical integrations, we use an exponential grid of the form

$$r(i) = r_0[e^{(i-1)h} - 1], \tag{17}$$

considering the grid size $h = 0.03125$, $r_0 = 0.0005$ and the total number of grids as 500.

Similarly, it is also very important to determine the dynamic polarizabilities of the atoms very accurately at all the frequencies for the above purpose. Since it requires sophisticated many-body methods for their calculations, it is difficult to evaluate them precisely for a large number of frequencies. In addition, the *ab initio* methods may not give very accurate results attributing to the fact that there is an inclusion of the uncertainties from the calculated energy values along with errors associated with the calculated $E1$ matrix elements and these calculations need to be performed repeatedly for all the frequencies which is, in fact, a tedious procedure. To avoid such calculations, the dynamic polarizabilities of an atom are estimated approximately in the evaluation of C_3 coefficients using single oscillator model as [24]

$$\alpha(\iota\omega) = \frac{\alpha(0)}{1 + \frac{\omega^2}{\omega_o^2}}, \tag{18}$$

where $\alpha(0)$ is the static dipole polarizability and ω_0 is the characteristic frequency used in the Lorentz oscillator model at the infrared absorption of the atom. However, to obtain precision in our results we use a different method to calculate these frequency-dependent polarizabilities which is briefly described below.

Methods to calculate atomic wave functions for the alkali-metal atoms are well established now and the $E1$ matrix elements of the principal transitions have been determined precisely [19,20,34,35]. It is, therefore, possible to evaluate the major part of the dynamic polarizabilities by combining these matrix elements with the experimental energies very accurately in a sum-over-states approach and the other nondominant contributions can be estimated in an *ab initio* approach using lower order many-body methods. Below, we describe briefly the procedure adopted in the present work for the calculations of the dynamic dipole polarizabilities in the considered atoms.

The dynamic dipole polarizability of a state $|\Psi_n\rangle$ in an atom is given by

$$\begin{aligned}\alpha(\omega) &= \sum_I \left[\frac{|\langle\Psi_n|D|\Psi_I\rangle|^2}{E_I - E_n + \omega} + \frac{|\langle\Psi_n|D|\Psi_I\rangle|^2}{E_I - E_n - \omega}\right] \\ &= \frac{2}{3(2J_n+1)}\sum_I \frac{(E_I - E_n)|\langle\Psi_n||D||\Psi_I\rangle|^2}{(E_I - E_n)^2 - \omega^2},\end{aligned} \tag{19}$$

where $J_n = 1/2$ is the total angular momentum of the ground state, the sum over I represents all possible allowed intermediate states for the dipole transition, E's are the energies of the corresponding states, and $\langle\Psi_n||D||\Psi_I\rangle$ is the $E1$ reduced matrix element of the dipole operator D between the states $|\Psi_n\rangle$ and $|\Psi_I\rangle$ in the considered alkali-metal atoms. This expression can be rewritten as

$$\alpha(\omega) = \langle\Psi_n|D|\Psi_n^{(+)}\rangle + \langle\Psi_n|D|\Psi_n^{(-)}\rangle, \tag{20}$$

with

$$|\Psi_n^{(\pm)}\rangle = \sum_I |\Psi_I\rangle \frac{\langle\Psi_I|D|\Psi_n\rangle}{E_I - E_n \pm \omega}, \tag{21}$$

which are obtained here using the Dirac-Coulomb (DC) Hamiltonian (H^{DC}) by solving the equation

$$(H^{\mathrm{DC}} - E_n \mp \omega)|\Psi_n^{(\pm)}\rangle = -D|\Psi_n\rangle. \tag{22}$$

We divide various correlation contributions to α into three parts for their easy and accurate determination as

$$\alpha(\omega) = \alpha_c(\omega) + \alpha_{vc}(\omega) + \alpha_v(\omega), \tag{23}$$

where the subscripts c, vc, and v correspond to contributions from the core, core-valence, and valence correlations, respectively. As known before, $\alpha_v(\omega)$ is the principal contributing part in the ground states of the considered atoms [19,20,34,35] and they can be evaluated very accurately using the $E1$ matrix elements of the transitions from the ground state to low-lying excited states and the experimental energies. We use directly the sum-over-states formula of Eq. (19) to

TABLE I. Summary of the ground-state dipole polarizability results (in a.u.) of the considered alkali-metal atoms obtained from the high-precision calculations and experiments.

Method	Li	Na	K	Rb
Ours [34,35]	164.1(6)	162.4(2)	289.8(6)	318.3(6)
Refs. [20,40]		162.6(3)	290.2(8)	318.6(6)
Experiment	164.2(11) [37]	162.7(8) [38]	290.58(1.42) [39]	319.9(6.1) [20]

estimate α_v contributions explicitly from the intermediate states. Contributions from the high-lying excited states (given as tail contributions), and $\alpha_c(\omega)$ and $\alpha_{vc}(\omega)$ are estimated solving Eq. (22) using the DF method. Recently, we have demonstrated that the polarizability calculations using the DF method for the closed-shell configurations similar to the cores of the alkali-metal atoms are very close to the RRPA and RCC methods and estimate the results more accurately than the lower order many-body perturbation methods [36].

To calculate $E1$ matrix elements, we express the atomic wave function of the ground and low-lying excited states in the alkali-metal atoms with a valence electron v as

$$|\Psi_v\rangle = e^T\{1 + S_v\}|\Phi_v\rangle, \tag{24}$$

where $|\Phi_v\rangle$ is the DF wave function and T and S_v operators account the correlation effects to all orders through the excitations of the electrons from the core orbitals alone and from the valence orbital together from the core orbitals, respectively. We consider here all the nonlinear terms with all possible singly and doubly excited configurations with the important triply excited configurations in the CCSD(T) method framework.

The $E1$ reduced matrix elements between the states $|\Psi_f\rangle$ and $|\Psi_i\rangle$ have been evaluated using the RCC expression [34–36]

$$\langle\Psi_f||D||\Psi_i\rangle = \frac{\langle\Phi_f||\{1 + S_f^\dagger\}\overline{D}\{1 + S_i\}||\Phi_i\rangle}{\sqrt{\mathcal{N}_f\mathcal{N}_i}}, \tag{25}$$

where $\overline{D} = e^{T^\dagger}De^T$ and $\mathcal{N}_v = \langle\Phi_v|e^{T^\dagger}e^T + S_v^\dagger e^{T^\dagger}e^T S_v|\Phi_v\rangle$.

IV. RESULTS AND DISCUSSION

The $E1$ matrix elements used here are already given in our previous papers where we have determined dynamic polarizabilities for the considered atoms with real frequencies [34,35]. By combining these matrix elements with the experimental energies, we estimate here the $\alpha_v(\iota\omega)$ contributions. To verify the accuracies in our calculations, we present the static dipole polarizabilities in Table I calculated by us with the above $E1$ matrix elements and compare them with the results from the measurements and other highly precise calculations by Derevianko and coworkers [20,40]. We also plot the dynamic polarizabilities at imaginary frequencies from the present work and using the data from [40] in Fig. 1.

As can be seen from the table and figure, the agreement between the results is excellent. It is, therefore, expected that the dispersion coefficients for the perfect conductors will match in both the works. Substituting the dynamic

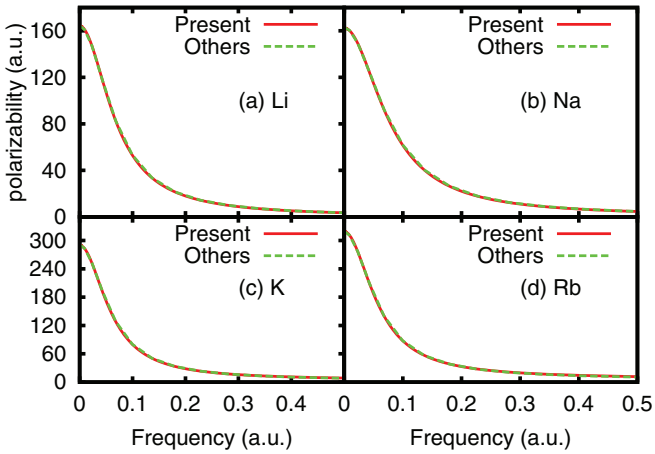

FIG. 1. (Color online) Comparison between the dynamic polarizabilities of the Li, Na, K, and Rb atoms against the results from Ref. [40] as "Others". The agreement between the results is excellent.

polarizabilities in Eq. (5) and comparing with Eq. (6), we evaluate the C_3 coefficients for a perfect conductor and the results for different atoms are presented in Table II which are compared with the results given in Refs. [20,40]. Even though the dynamic polarizabilities, as discussed above, appear to be in close agreement with each other, the differences in the estimated C_3 values are noticeable, especially, in the heavier atoms (5% larger for K and 8% larger for Rb). We owe part of the discrepancy to the numerical integration methods used in both the works. Derevianko and coworkers have used a Gaussian quadrature integration procedure with just fifty data points, whereas we use an exponential grid structure with 500 data points in our calculations. To see the sensitivity of the results with the choice of different grids, we instead used a linear grid having a spacing size 0.1 and observed a 3%–5% fall in C_3 coefficients for the considered atoms, the reason being that most of the contributions to these coefficients come from the lower frequencies which yield inaccuracy in the results with a large grid size. Moreover, we were unable to reproduce the results given in Ref. [40] using their integration technique given by Eq. (8) of Ref. [40] implying that the discrepancies arise mainly from the numerical methods employed in both the works. The differences in these results are more prominent from the ratios of the estimated C_3 values among various atoms that are given in Table III. The valence correlation contribute predominantly to the C_3 coefficients followed by the core correlations and they increase with the size of the atomic systems which are in accordance with the findings in [20,40]. We noticed that the tendency for the present calculations to give larger results for the C_3 coefficients of the atom-perfect conductor interaction was mainly coming from the core contributions. For example, the core correlation contributions are about 40% of the total C_3 of Rb atom in the present calculations in contrast to 35% in Ref. [20,40]. Our results are in excellent agreement with the findings made by Mitroy and coworkers [41], who have made similar observation regarding the C_3 values of Refs. [20]. To assure that the discrepancy in core contribution was not owing to the fact that Derevianko and coworkers have employed RRPA method for core calculations whereas we have used

TABLE II. Calculated C_3 coefficients along with their uncertainties for the alkali-metal atoms and their comparison with other reported values. Uncertainties from our calculations are given in the parentheses with no account to errors associated with the optical data used for the material media. Classification of various contributions is in accordance with [19][a], [20][b], [40][c], [41][d], and [22][e].

	Li	Na	K	Rb
		Perfect Conductor		
Core	0.074	0.332	0.989	1.513
Valence	1.387	1.566	2.115	2.254
Core-Valence	∼0	∼0	−0.016	−0.028
Tail	0.055	0.005	0.003	0.003
Total	1.516(2)	1.904(2)	3.090(4)	3.742(5)
Others	1.5178[a]	1.8858[b]	2.860[b]	3.362[b]
	1.512[c]	1.871[c]	2.896[c]	3.426[c]
	1.521[d]	1.931[d]	3.017[d]	3.633[d]
		1.889[e]		
		Metal: Au		
Core	0.010	0.051	0.263	0.419
Valence	1.160	1.285	1.804	1.927
Core-Valence	∼0	∼0	−0.005	−0.010
Tail	0.029	0.002	0.001	0.002
Total	1.199(2)	1.338(1)	2.062(4)	2.338(4)
Others [23]	1.210(5)	1.356(6)	2.058(9)	2.31(1)
		Semiconductor: Si		
Core	0.006	0.033	0.184	0.299
Valence	0.993	1.099	1.543	1.649
Core-Valence	∼0	∼0	−0.004	−0.008
Tail	0.023	0.002	0.001	0.001
Total	1.022(2)	1.134(1)	1.724(3)	1.942(4)
		Dielectric: SiO_2		
Core	0.004	0.022	0.116	0.184
Valence	0.468	0.519	0.726	0.775
Core-Valence	∼0	∼0	−0.002	−0.004
Tail	0.012	0.001	0.001	0.001
Total	0.4844(8)	0.5424(5)	0.839(1)	0.956(2)
		Dielectric: SiN_x		
Core	0.005	0.024	0.138	0.224
Valence	0.710	0.788	1.101	1.176
Core-Valence	∼0	∼0	−0.003	−0.006
Tail	0.017	0.001	0.001	0.001
Total	0.715(1)	0.7939(8)	1.212(2)	1.369(3)
Experiment [16]		0.67(20)		

DF method, we repeated our calculations using RRPA values for core and found that our C_3 values do not change much (see Ref. [36] to learn of similar observations in the dipole polarizability calculations).

We plot $\epsilon(\iota\omega)$ values of all the considered materials against the frequencies in Fig. 2. The behavior of $\epsilon(\iota\omega)$ for various materials are seen to be in accordance with the graphical representations given by Caride and coworkers [24]. To summarize, these values are very large for Au in low-frequency regime and then fall sharply with a long tail in the asymptotic region. The values for Si follow that of Au with

TABLE III. Comparison of the ratios of the C_3 coefficients for the alkali-metal atoms in different media.

	C_3^{Li}/C_3^{Na}	C_3^{K}/C_3^{Na}	C_3^{Rb}/C_3^{K}	C_3^{Rb}/C_3^{Na}
		Perfect Conductor		
This work	0.796(3)	1.623(5)	1.211(6)	1.965(5)
Ref. [20]	0.805[a]	1.517	1.176	1.783
Ref. [40]	0.808	1.548	1.183	1.831
		Metal: Au		
This work	0.896(2)	1.541(4)	1.334(6)	1.747(4)
Ref. [23]	0.892(8)	1.518(11)	1.122(13)	1.704(12)
		Semiconductor: Si		
This work	0.901(2)	1.520(3)	1.126(5)	1.713(4)
		Dielectric: SiO_2		
This work	0.893(1)	1.547(1)	1.139(2)	1.763(2)
		Dielectric: SiN_x		
This work	0.900(2)	1.527(4)	1.129(4)	1.724(6)
Experiment [17]	0.89(4)	1.544(25)	1.12(4)	1.724(7)

[a]Obtained by combining results from [19] and [20].

$\epsilon(0)$ corresponding to 11.64. The dielectric materials have very slow varying dielectric constants with $\epsilon(0)$ values as 4.72 and 3.78 for SiO_2 and SiN_x, respectively. This plot also suggests that among both the dielectric materials, SiO_2 is supposed to interact with atoms more weakly than SiN_x.

We now present our calculated C_3 coefficients for the material media in Table II below the results for the perfect conductors. Uncertainties from the calculations are quoted in the parentheses with no account of errors from the used experimental data. This indicates the preciseness in the calculations of the C_3 coefficients for the perfect medium. The results for the considered material media can be improved further by reducing the uncertainties in the available optical data. These results are also compared with the values reported by other calculations and experimental values in the same table. Lach *et al.* [23] have evaluated the C_3 coefficients for Au. In their calculation the dielectric constants were evaluated using the Drude model and Drude-Lorentz functions and the

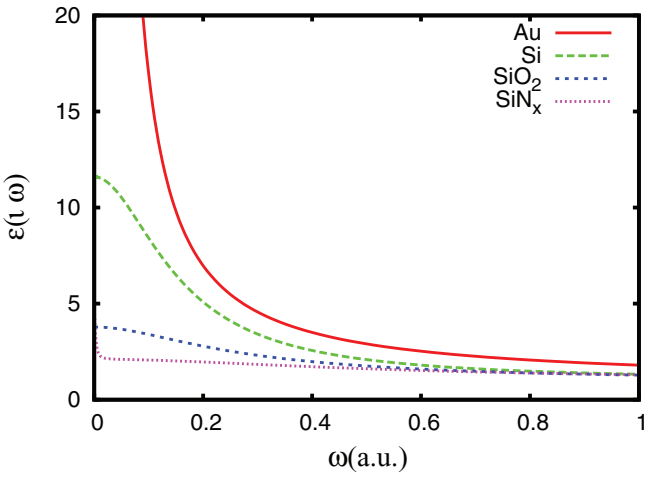

FIG. 2. (Color online) Imaginary dynamic dielectric constants of the Au, Si, SiO_2, and SiO_2 surfaces along the imaginary axis as functions of frequencies.

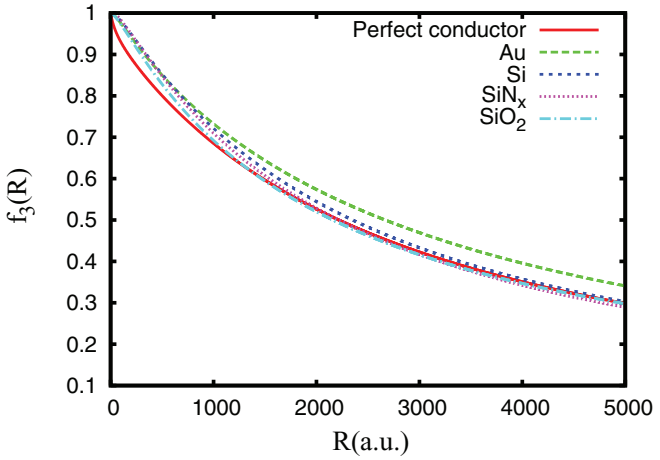

FIG. 3. (Color online) The retardation coefficient $f_3(R)$ for Li atom as a function of distance R from different walls.

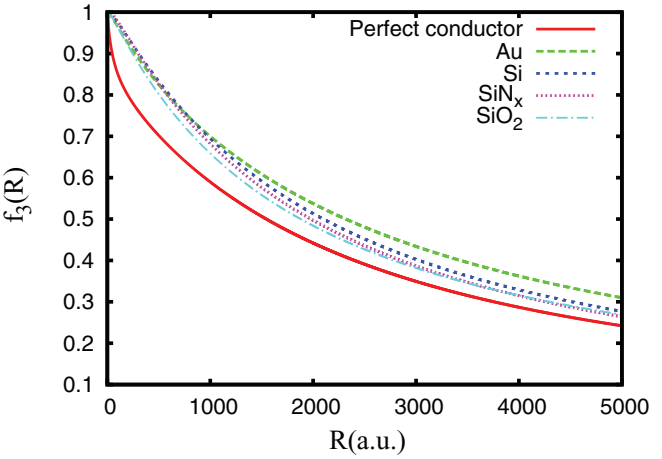

FIG. 4. (Color online) The retardation coefficient $f_3(R)$ for Na atom as a function of distance R from different walls.

dynamic polarizabilities were taken from Ref. [20]. We find there is a significant difference in both the calculations which may be arising from the fact that dynamic polarizabilities and dielectric constants used were calculated using different methods. There is only one experimental result available for the Na atom–SiN_x wall as 0.67(20) [22] which has a very large uncertainty associated with it and hence cannot really test the accuracy of our calculation. Also, the C_3 coefficients for a perfect conductor are approximately 1.5, 2, 2.5, and 3.5 times larger than the Au, Si, SiN_x, and SiO_2 media, respectively. The decrease in the coefficient values in the material media can be attributed to the fact that in case of the dielectric material the theory is modified for nonunity reflection and for different origin of the transmitted waves from the surface [10,11]. There are also additional interactions in Si, SiN_x, and SiO_2 due to charge dangling bonds at the shorter separations [42].

We also calculate ratios of the C_3 coefficients for all the considered atoms in different materials and present them in Table III. The purpose of giving these values is to verify the corresponding experimental results for the SiN_x material reported in [17,18] as well as to investigate their trends. We find a very good agreement between our results with the measured values, given in the above table, for all the cases. However, these ratios are different from the ratios that we have obtained for the perfect conductors given in the same table. Lonij *et al*. have argued in [17,18], by extrapolating their results using a Lorentz oscillator model and assuming very large surface-plasmon frequency near the surface of SiN_x, that their measurements support the results reported in [20] for the perfect conductor. In a recent work, we have shown that the Lorentz oscillator model over estimates the dynamic polarizabilities in the alkali-metal atoms [43], especially in the heavy atoms like K and Rb. Therefore, agreement of the experimental results with the estimated values of Ref. [20] may be accidental. Our calculations do not take into account any of these assumptions and agreement of our results with the measurements are based purely on the findings from the calculations. We also notice that the ratios of the C_3 coefficients among different materials for the alkali-metal atoms vary slowly. More precise measurements of these ratios in all the considered materials will be very useful to test the validity of our results.

In Figs. 3–6, we show a comparison of the $f_3(R)$ values obtained for the Li, Na, K, and Rb atoms as functions of the atom-wall separation distance R for the undertaken four different materials studied in this work. As seen in these figures, the retardation coefficients are the smallest for an ideal metal. At very short separation distances the results for a perfectly conducting material differ from the results of Au, Si, SiN_x, and SiO_2 by less than 4%. As the atom-surface distance increases, the deviations of $f_3(R)$ results for various materials from the results of an ideal metal are considerably large and vary about 18%, 15%, and 6% for Li; 33%, 14%, and 18% for Na; 40%, 13%, and 26% for K; and 50%, 13%, and 33% for Rb in Au, Si and SiN_x, and SiO_2 surfaces, respectively. The deviations of the results between an ideal metal and other dielectric surfaces are minimum for the Li atom and they increase appreciably for the Rb atom. We use a functional form to describe the above atom-wall retarded interaction potentials

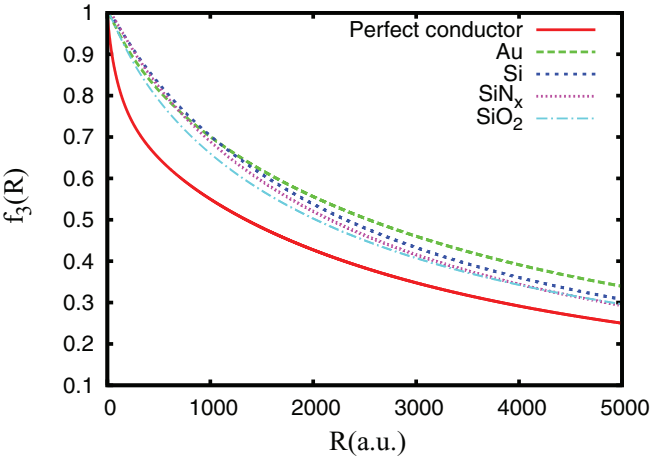

FIG. 5. (Color online) The retardation coefficient $f_3(R)$ for K atom as a function of distance R from different walls.

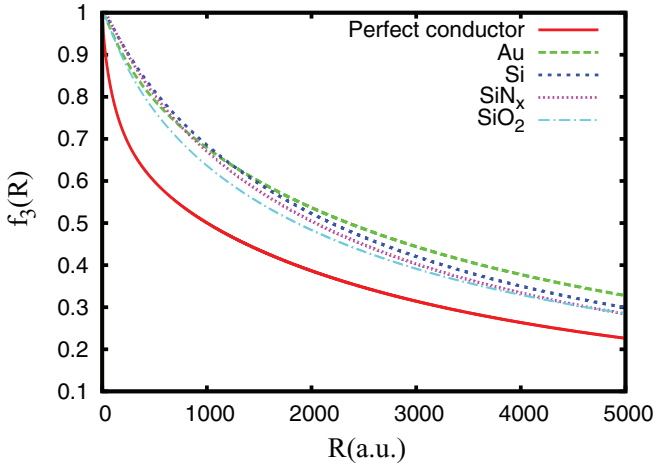

FIG. 6. (Color online) The retardation coefficient $f_3(R)$ for Rb atom as a function of distance R from different walls.

at the separate distance R as

$$f_3(R) = \frac{1}{a + b(\alpha_{fs} R)}. \tag{26}$$

We calculate $f_3(R)$ values substituting frequency-dependent atomic polarizabilities and dielectric constants of the materials in Eq. (1) and then comparing it with Eq. (3). By fitting the obtained data into the expression given above, we find the a and b values for the considered atoms in all the materials which are listed in Table IV.

In Table V, we present our calculated results for the C_6 coefficients of the alkali-metal dimers. In the second, third, and fourth columns, we give individual contributions from the valence, core, and valence-core polarizabilities to C_6 evaluation, and the fifth column contains contributions from the cross terms from various correlations which are found to be crucial for obtaining accurate results. As can be seen from Tables II and V, the trends of contributions from various correlations are almost similar in the C_3 and C_6 evaluations. A comparison of our C_6 values with other recent calculations and available experimental results is also presented in the same table. Our results are in very good agreement with the results reported in [40,44] except for the K-Rb heteronuclear dimer and in some cases the uncertainties reported in both the works tightly constraint these values. We plot the estimated $f_6(R)$ parameters for the homonuclear and the heteronuclear dimers in Figs. 7 and 8, respectively. Our plot for the homonuclear dimers is in very close agreement with Fig. 2 of [45] although there are slight changes in the values due to the use of different polarizabilities in both the works. Using a fitting procedure similar to that for f_3, we obtained fitting parameters a and b for these $f_6(R)$ functions and quote them in the last two columns of Table V.

TABLE IV. Fitting parameters a and b for f_3 coefficients with a perfectly conducting wall, Au, Si, SiO_2, and SiN_x surfaces.

	Li	Na	K	Rb
		Perfect Conductor		
a	0.9843	1.0802	1.1845	1.2598
b	0.0676	0.0866	0.0808	0.0907
		Metal: Au		
a	0.9775	0.9846	1.0248	1.0437
b	0.0675	0.0614	0.0532	0.0558
		Semiconductor: Si		
a	0.9436	0.9436	0.9749	0.9869
b	0.0638	0.0718	0.0622	0.0647
		Dielectric: SiO_2		
a	0.9754	0.9789	1.0238	1.0423
b	0.0650	0.0746	0.0649	0.0685
		Dielectric: SiN_x		
a	0.9380	0.9376	0.9712	0.9833
b	0.0680	0.0766	0.0668	0.0696

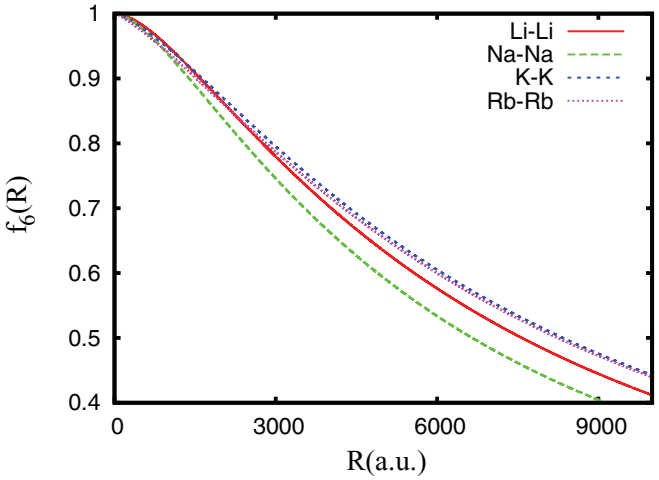

FIG. 7. (Color online) The retardation coefficient $f_6(R)$ for the homonuclear alkali-metal dimers as a function of atom-atom distance R.

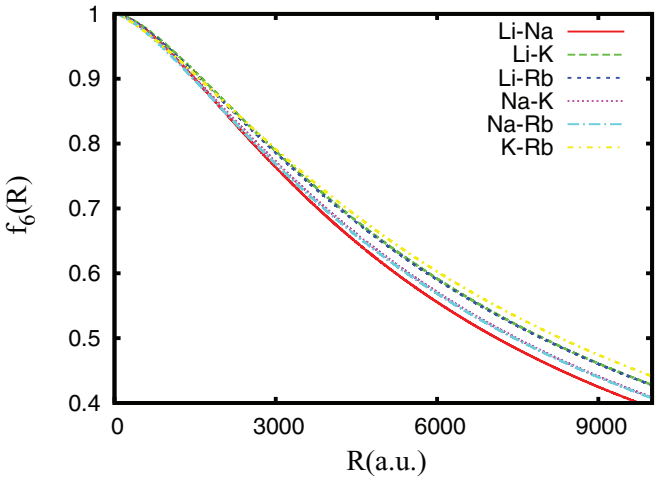

FIG. 8. (Color online) The retardation coefficient $f_6(R)$ for the heteronuclear alkali-metal dimers as a function of atom-atom distance R.

TABLE V. C_6 coefficients with fitting parameters for the alkali-metal dimers. Contributions from the valence, core, and valence-core polarizabilities alone are labeled as C_6^v, C_6^c, and C_6^{vc}, respectively, and C_6^{ct} corresponds to contributions from the remaining cross terms. References: [a][40,44], [b][45], [c][41], [d][46], [e][47], [f][48], [g][49].

Dimer	C_6^v	C_6^c	C_6^{vc}	C_6^{ct}	C_6 (Total)	Others	Exp.	a	b
Li-Li	1351	0.07	∼0	39	1390(4)	1389(2)[a], 1388[b], 1394.6[c], 1473[d]		0.8592	0.0230
Li-Na	1428	0.32	∼0	37	1465(3)	1467(2)[a]		0.8592	0.0245
Li-K	2201	1.27	∼0	119	2321(6)	2322(5)[a]		0.8640	0.0217
Li-Rb	2368	1.94	∼0	179	2550(6)	2545(7)[a]		0.8666	0.0262
Na-Na	1515	1.51	∼0	33	1550(3)	1556(4)[a], 1472[b], 1561[c]		0.8591	0.0262
Na-K	2316	6.24	∼0	118	2441(5)	2447(6)[a]	2519[e]	0.8555	0.0231
Na-Rb	2490	9.60	∼0	184	2684(6)	2683(7)[a]		0.8686	0.0232
K-K	3604	29.89	0.01	261	3895(15)	3897(15)[a], 3813[b], 3905[c]	3921[f]	0.8738	0.0207
K-Rb	3880	46.91	0.02	465	4384(12)	4274(13)[a]		0.8738	0.0207
Rb-Rb	4178	73.96	0.4	465	4717(19)	4691(23)[a], 4426[b], 4635[c]	4698[g]	0.8779	0.0207

V. CONCLUSION

To summarize, we have investigated the dispersion and damping coefficients for the atom-wall and atom-atom interactions for the Li, Na, K, and Rb atoms and their dimers in this work. Although our dynamic polarizability results are in agreement with the previous calculations, the estimated dispersion coefficients using these values differ. We have also studied the interaction coefficients of the above alkali-metal metals considering the wall surfaces made up of Au, Si, SiN_x, and SiO_2 materials. These results are compared against the values obtained for a perfect conductor and other available data. The errors of our results originating from the inaccuracies of atomic dynamic polarizabilities are smaller than in previously calculated values. The ratios of the dispersion coefficients among different atoms for various material media are almost constant while their absolute values are highly material dependent. Precise measurements of these ratios among the considered alkali-metal atoms in different material media will be able to test the validity of the theoretical results. Readily usable functional forms of the retardation coefficients for the interaction between two alkali-metal atoms and alkali-metal atoms with the above media are provided. Our fit explains more than 99% of total variation in data from the average.

ACKNOWLEDGMENTS

The work of B.A. is supported by the CSIR, India (Grant No. 3649/NS-EMRII). We thank Dr. G. Klimchitskaya and Dr. G. Lach for some useful discussions. B.A. also thanks S. Sokhal for his help in some calculations. Computations were carried out using the 3TFLOP HPC Cluster at Physical Research Laboratory, Ahmedabad.

[1] E. M. Lifshitz and L. P. Pitaevskii, *Statistical Physics* (Pergamon Press, Oxford, 1980).
[2] H. B. G. Casimir and D. Polder, Phys. Rev. **73**, 360 (1948).
[3] F. London, Z. Physik **63**, 245 (1930).
[4] J. Israelachvili, *Intermolecular and Surface Forces* (Academic Press, San Diego, 1992).
[5] M. Antezza, L. P. Pitaevskii, and S. Stringari, Phys. Rev. A **70**, 053619 (2004).
[6] R. Folman, P. Krüger, D. Cassettari, B. Hessmo, T. Maier, and J. Schmiedmayer, Phys. Rev. Lett. **84**, 4749 (2000).
[7] J. L. Roberts, N. R. Claussen, J. P. Burke, C. H. Greene, E. A. Cornell, and C. E. Wieman, Phys. Rev. Lett. **81**, 5109 (1998).
[8] C. Amiot and J. Verges, J. Chem. Phys. **112**, 7068 (2000).
[9] P. J. Leo, C. J. Williams, and P. S. Julienne, Phys. Rev. Lett. **85**, 2721 (2000).
[10] D. M. Harber, J. M. McGuirk, J. M. Obrecht, and E. A. Cornell, J. Low Temp. Phys. **133**, 229 (2003).
[11] D. M. Harber, Ph.D. thesis, University of Colorado, 2005.
[12] A. E. Leanhardt, Y. Shin, A. P. Chikkatur, D. Kielpinski, W. Ketterle, and D. E. Pritchard, Phys. Rev. Lett. **90**, 100404 (2003).
[13] Y. Lin, I. Teper, C. Chin, and V. Vuletić, Phys. Rev. Lett. **92**, 050404 (2004).
[14] A. Aspect and J. Dalibard, *Poincare Seminar*, edited by B. Duplantier and V. Rivasseau (Birkhäuser Verlag, Basel, 2003).
[15] R. Brühl, P. Fouquet, R. E. Grisenti, J. P. Toennies, G. C. Hegerfeldt, T. Köhler, M. Stoll, and C. Walter, Europhys. Lett. **59**, 357 (2002).
[16] J. D. Perreault, A. D. Cronin, and T. A. Savas, Phys. Rev. A **71**, 053612 (2005).
[17] V. P. A. Lonij, C. E. Klauss, W. F. Holmgren, and A. D. Cronin, Phys. Rev. Lett. **105**, 233202 (2010).
[18] V. P. A. Lonij, C. E. Klauss, W. F. Holmgren, and A. D. Cronin, J. Phys. Chem. A **115**, 7134 (2011).
[19] A. Derevianko, W. R. Johnson, and S. Fritzsche, Phys. Rev. A **57**, 2629 (1998).
[20] A. Derevianko, W. R. Johnson, M. S. Safronova, and J. F. Babb, Phys. Rev. Lett. **82**, 3589 (1999).
[21] J. Jiang, Y. Cheng, and J. Mitroy, J. Phys. B **46**, 125004 (2013).
[22] P. Kharchenko, J. F. Babb, and A. Dalgarno, Phys. Rev. A **55**, 3566 (1997).
[23] G. Lach, M. Dekieviet, and U. D. Jentschura, Int. J. Mod. Phys. A **25**, 2337 (2010).
[24] A. O. Caride, G. L. Klimchitskaya, V. M. Mostepanenko, and S. I. Zanette, Phys. Rev. A **71**, 042901 (2005).

[25] J. F. Babb, G. L. Klimchitskaya, and V. M. Mostepanenko, Phys. Rev. A **70**, 042901 (2004).
[26] A. Lambrecht, I. Pirozhenko, L. Duraffourg, and Ph. Andreucci, Eur. Phys. Lett. **77**, 44006 (2007).
[27] S. Y. Buhmann, L. Knöll, D.-G. Welsch, and H. T. Dung, Phys. Rev. A **70**, 052117 (2004).
[28] V. B. Bezerra, G. L. Klimchitskaya, V. M. Mostepanenko, and C. Romero, Phys. Rev. A **78**, 042901 (2008).
[29] G. Bimonte, G. L. Klimchitskaya, and V. M. Mostepanenko, Phys. Rev. A **79**, 042906 (2009).
[30] E. M. Lifshitz, Zh. Eksp. Teor. Fiz. **29**, 94 (1955) [JETP **2**, 73 (1956)].
[31] S. Y. Buhmann, H. T. Dung, T. Kampf, and D.-G. Welsch, Eur. Phys. J. D **35**, 15 (2005).
[32] See http://www.wolfram.com/mathematica.
[33] E. D. Palik, *Handbook of Optical Constants of Solids* (Academic Press, San Diego, 1985).
[34] B. Arora and B. K. Sahoo, Phys. Rev. A **86**, 033416 (2012).
[35] B. K. Sahoo and B. Arora, Phys. Rev. A **87**, 023402 (2013).
[36] Y. Singh, B. K. Sahoo, and B. P. Das, Phys. Rev. A **88**, 062504 (2013).
[37] A. Miffre, M. Jacquey, M. Büchner, G. Trenec, and J. Vigue, Eur. Phys. J. D **38**, 353 (2006).
[38] C. R. Ekstrom, J. Schmiedmayer, M. S. Chapman, T. D. Hammond, and D. E. Pritchard, Phys. Rev. A **51**, 3883 (1995).
[39] W. F. Holmgren, M. C. Revelle, V. P. A. Lonij, and A. D. Cronin, Phys. Rev. A **81**, 053607 (2010).
[40] A. Derevianko, S. G. Porsev, and J. F. Babb, At. Data Nucl. Data Tables **96**, 323 (2010).
[41] J. Mitroy and M. W. J. Bromley, Phys. Rev. A **68**, 052714 (2003).
[42] A. S. Foster, A. Y. Gal, J. D. Gale, Y. J. Lee, R. M. Nieminen, and A. L. Shluger, Phys. Rev. Lett. **92**, 036101 (2004).
[43] B. Arora, H. Kaur, and B. K. Sahoo, arXiv:1311.7537.
[44] A. Derevianko, J. F. Babb, and A. Dalgarno, Phys. Rev. A **63**, 052704 (2001).
[45] M. Marinescu, H. R. Sadeghpour, and A. Dalgarno, Phys. Rev. A **49**, 982 (1994).
[46] L. W. Wansbeek, B. K. Sahoo, R. G. E. Timmermans, B. P. Das, and D. Mukherjee, Phys. Rev. A **78**, 012515 (2008); **82**, 029901(E) (2010).
[47] I. Russier-Antoine, A. J. Ross, M. Aubert-Frecon, F. Martin, and P. Crozet, J. Phys. B **33**, 2753 (2000).
[48] A. Pashov, P. Popov, H. Knöckel, and E. Tiemann, Eur. Phys. J. D **46**, 241 (2008).
[49] C. Chin, V. Vuletić, A. J. Kerman, S. Chu, E. Tiesinga, P. J. Leo, and C. J. Williams, Phys. Rev. A **70**, 032701 (2004).